

Cheng Liu,[†] Mary C. McKinney,[‡] Yi-Hsing Chen,[§] Tyler M. Earnest,[†] Xinghua Shi,^{**} Li-
Jung Lin,[§] Yoshizumi Ishino,^{††} Karin Dahmen,[†] Isaac K. O. Cann,^{§¶||} and Taekjip
Ha^{†‡¶||***}

[†]Department of Physics and the Center for the Physics of Living Cells, [‡]Center for Biophysics and
Computational Biology, [§]Department of Animal Sciences, [¶]Institute for Genomic Biology and ^{||}Department
of Microbiology, University of Illinois at Urbana-Champaign, Champaign, Illinois; ^{**}Howard Hughes
Medical Institute, Urbana, Illinois; and ^{††}Department of Genetic Resources, Faculty of Agriculture, Kyushu
University, Fukuoka-shi, Japan

Supplementary Methods

DNA constructs and annealing protocol.

Annealing of DNA constructs was performed in a 20mM Tris (pH 8.0) and 200mM NaCl buffer. The sample was heated to 90°C for 10 minutes and then left to cool to room temperature over many hours in the dark. The 4WJ-DNA was gel purified in an 8% native acrylamide gel. The sequence for the pdDNA's are
Primer: 5' -Biotin- TGGCGACGGCAGCGAGGC -Cy5
Template: 5' T₄₀ GCCTCGCTGCCGTCGCCA.

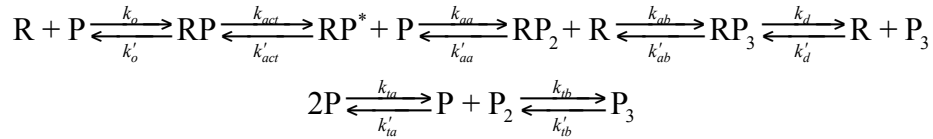
The DNA's for the 4WJ-DNA are:

5'-CCCTAGCAAGCCGCTGCTACGG or 5'-Cy5-CCCTAGCAAGCCGCTGCTACGG,
5'- CCGTAGCAGCGCAGCGGTGGG, 5'- CCCACCGCTCGGCTCAACTGGG, 5'-
CCCAGTTGAGCGCTTGTAGGG T₂₀ CTCGGTTCTCGGGGATCCTATACTTGT,
and 5'-Biotin-ACAAGTATAGGATCCCCGAGAACCGAG-Cy5 or 5'-Biotin-
ACAAGTATAGGATCCCCGAGAACCGAG.

The DNA Template for pdDNA-b is: 5'-Biotin-T₁₀ GCCTCGCTGCCGTCGCCA.

Kinetic modeling of PCNA assembly dynamics

To fit the ensemble FRET data to the proposed model (Figure S6), we used the following model.



To keep track of the donor and acceptor labels, two separate PCNA monomer species, P' and P'' are introduced. We follow the procedure of Brown and Sethna. [1] The chemical rate equations are integrated and the concentration time courses for all species that contain two different labels are summed. This is proportional to the FRET signal only in approximation. The FRET efficiencies are not the same for each donor-acceptor pair because the species P'P'P'' and P''P'P'' would not in general have the same FRET efficiency. Labeling efficiency is also neglected.

The chemical rate equations are integrated using the CVODE package. [2] The chemical equations are entered into a text file using shorthand. The text file is parsed with a Perl script to produce C code for both the ODE right hand side function and the Jacobian. The derivatives are calculated using Maxima. Since there are 27 separate chemical reactions, 14 rate constants, and 21 different chemical species, this method greatly decreases the amount of time to write code and eliminates many possibilities for error. The parameters determined from the fitting are presented in Table S3.

Since the initial conditions are different for the self-assembly and assisted assembly experiments, they must be treated separately. For self-assembly, P' was added first to a buffer from a 4000 nM stock solution, allowed to equilibrate for 5 minutes, then P'' was added and data collection started. Thus the fraction of monomer, dimer, and trimer for P' are different than for P''. To account for this, the initial concentrations at equilibrium for

the two different PCNA concentrations were determined by solving the cubic equilibrium equations.

The preparation of the assisted assembly experiments was more complicated. First stock P' is added to the buffer. Then 5 minutes later stock P'' is added. After 15 minutes RFC is added and the data collection begins. The initial conditions were determined by simply following this schedule and using the ODE system to re-equilibrate for the time required.

To determine the goodness of fit, the cost function

$$C(\{\theta_j\}) = \sum_{f=1}^{N^{\text{ex}}} \mathcal{N}_f C_f^{\chi^2}(\{\theta_j\}) + \sum_{j=1}^{N^k} C_j^{\text{ct}}(\theta_j) + C^{\text{mag}}(\{\theta_j\}) + C^{\text{dim}}(\{\theta_j\}) + C^{\text{ccr}}(\{\theta_j\})$$

was used. Since the rate constants span many different orders of magnitude, it is sensible to write the cost function as a function of the logarithm of the rate constants $\theta_i = \ln k_i$.

The first term is the standard least squares term,

$$C_f^{\chi^2}(\{\theta_j\}) = \sum_{i=1}^{N^{\text{im}}} [F_f(t_i) - A_f y_f(t_i; \{\theta_j\})]^2$$

summed over all N^{ex} experimental conditions. Here $F_f(t_i)$ is the experimental FRET signal at experimental concentrations f at time t_i , $y_f(t_i; \{\theta_j\})$ is the predicted concentration evaluated at time t_i with parameters $\{\theta_j\}$, and A_f is a concentration to signal calibration constant (Table S4) determined by setting the A_f derivative of the cost function to zero and solving

$$A_f = \frac{\sum_{i=1}^{N_i(f)} F_f(t_i) y_f(t_i)}{\sum_{i=1}^{N_i(f)} [y_f(t_i)]^2}$$

The normalization \mathcal{N}_f is a normalization factor to ensure that each experiment is considered equally regardless of signal magnitude. Specifically,

$$\mathcal{N}_f = \frac{1}{N^{\text{ex}} N_f^{\text{im}} F_f(\infty)^2}$$

where N^{ex} is the total number of experimental time courses considered, N_f^{im} is the number of times the FRET signal was measured for experiment f , and $F_f(\infty)$ is the steady state FRET signal estimated by the average of the highest 10% of signal values.

The second term in the cost function is a sum over constraint functions evaluated for each rate constant to force the solution to take on reasonable values. It is legitimate to do this since the 14 rate constants are not all independent. There exist certain subspaces of the total parameter space that possess equal cost function value. These constraint functions just push the solver through these subspaces, leading to physically acceptable parameters. The constraint functions take the form

$$C^{\text{ct}}(\theta_j) = \begin{cases} M_j(\theta_{0,j} - \theta_j)^{\alpha_j}, & \theta_j < \theta_{0,j} \\ 0, & \theta_{0,j} \leq \theta_j \leq \theta_{1,j} \\ M_j(\theta_j - \theta_{1,j})^{\alpha_j}, & \theta_j > \theta_{1,j} \end{cases}$$

where θ_0 and θ_1 are the minimum and maximum acceptable log rate constants, and M and α determine the shape of the function. Outside of bounds the constraint function will have a steep gradient in the direction that corrects the rate constants and inside the bounds the constraint function contributes nothing to the cost function.

The third and fourth terms impose two experimental facts. The third term imposes that upon addition of 40 nM of RFC, a 40 nM solution of PCNA (1:1 labeling), the FRET signal jumps by 20x over a few minutes. The form of this term is the same as the C^{ct} terms, where we compare $\ln y_i(\infty)/y_i(0)$ at i corresponding to $[\text{RFC}] = 40 \text{ nM}$, $[\text{PCNA}] = 40 \text{ nM}$. The fourth term imposes that the concentration of dimers is very low. Again using the same form, the ratio of the concentration of FRET active dimers to FRET active trimers is compared at $t=\infty$.

The last term penalizes large ranges in the calibration constants. Since the self-assembly data were taken using the same PCNA stock, buffer, incubation times, and experimenter, it is reasonable to assume that the distribution of calibration constants should have a small range compared to the average. Since the self-assembly and assisted assembly data were collected under different conditions, the ranges are considered separately. Using the same form as the other constraints we test the value

$$\frac{\max A_i - \min A_i}{\langle A \rangle}$$

for each experiment separately.

The cost function is minimized using simulated annealing and quenched using the Nelder-Mead algorithm. [3] The minimum value of the cost function was 43.3%. The error was dominated by the C^{ccr} term for self-assembly (33.7%).

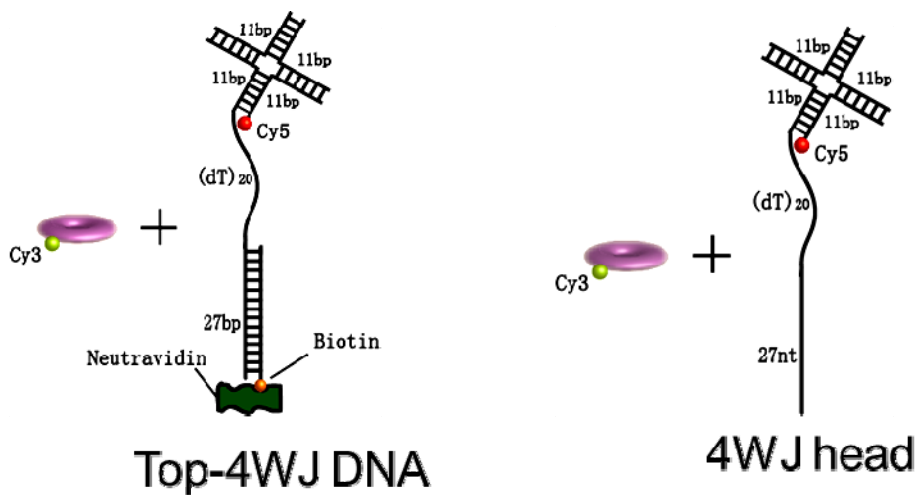
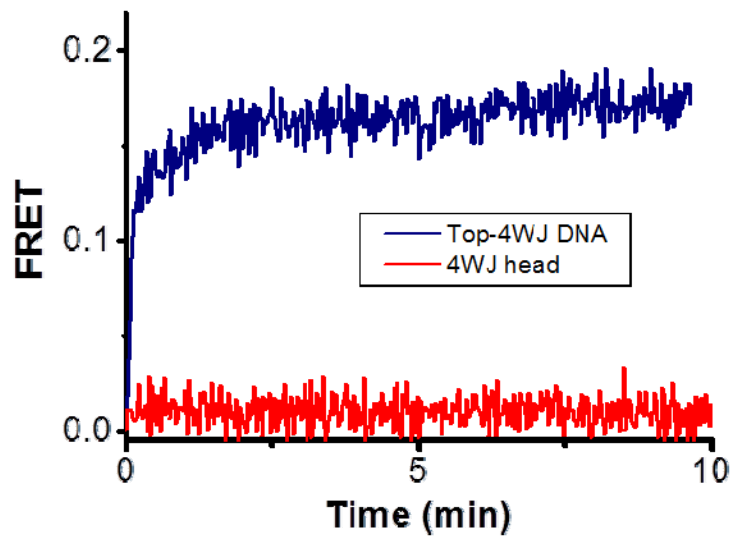
[1] K. S. Brown and J. S. Sethna Phys. Rev. E **68**, 021904 (2003)

[2] A. C. Hindmarsh, P. N. Brown, K. E. Grant, S. L. Lee, R. Serban, D. E. Shumaker, and C. S. Woodward ACM T. Math. Software **31**(3), 363 (2005)

[3] M. Galassi, J. Davies, J. Theiler, B. Gough, G. Jungman, P. Alken, M. Booth, F. Rossi, *GNU Scientific Library Reference Manual*, 3rd Ed. (Network Theory Ltd., United Kingdom, 2009)

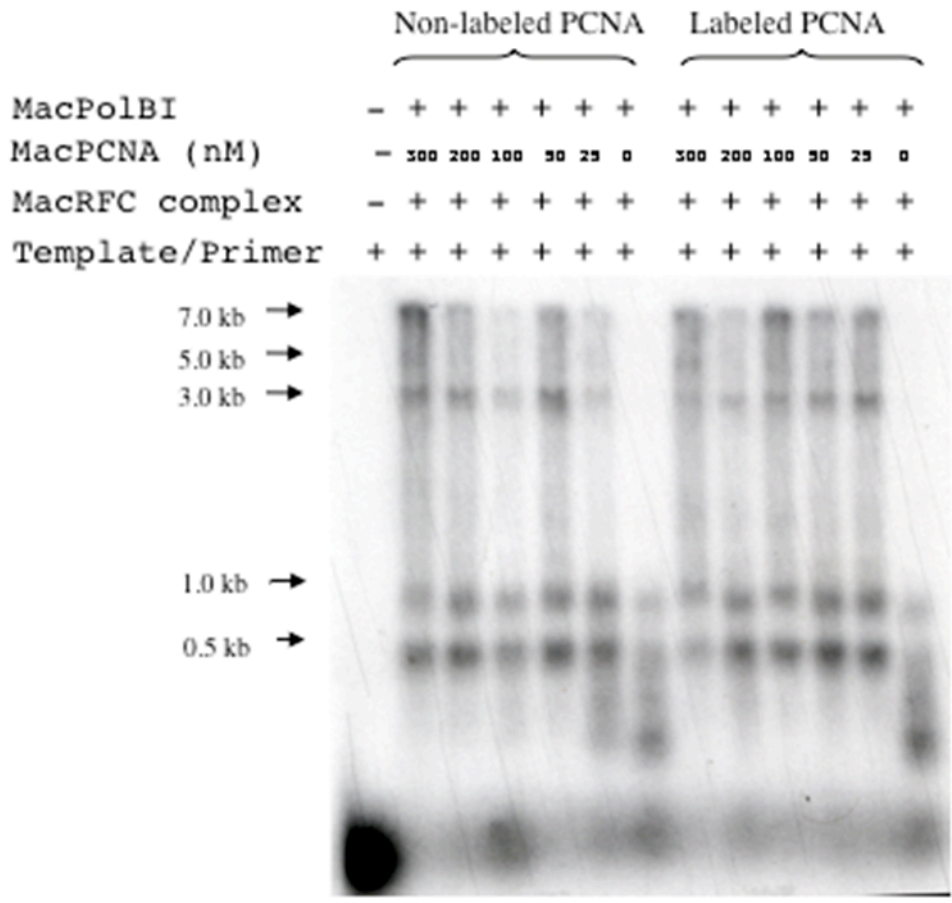
Supplementary Figure S1.

Control experiments for the loading of Cy3-labeled PCNA onto Cy5-labeled 4WJ-DNA DNA constructs were prepared to see if PCNA binding to the blunt ends of the four-way junction DNA may contribute to the FRET signal observed in our PCNA loading experiments. The data show negligible FRET increase for the four-way junction alone whereas a robust FRET increase was observed with the construct that contains the 3' recessed end.



Supplementary Figure S2.

Control experiments for the primer extension facilitation by Cy3-labeled PCNA
 Comparison of labeled and non-labeled MacPCNA on primer extension. Primer extension of MacPolBI was compared in the presence of different amount of labeled and non-labeled PCNA. The results indicated that labeled PCNA retains its function to accompany the polymerase during DNA synthesis.

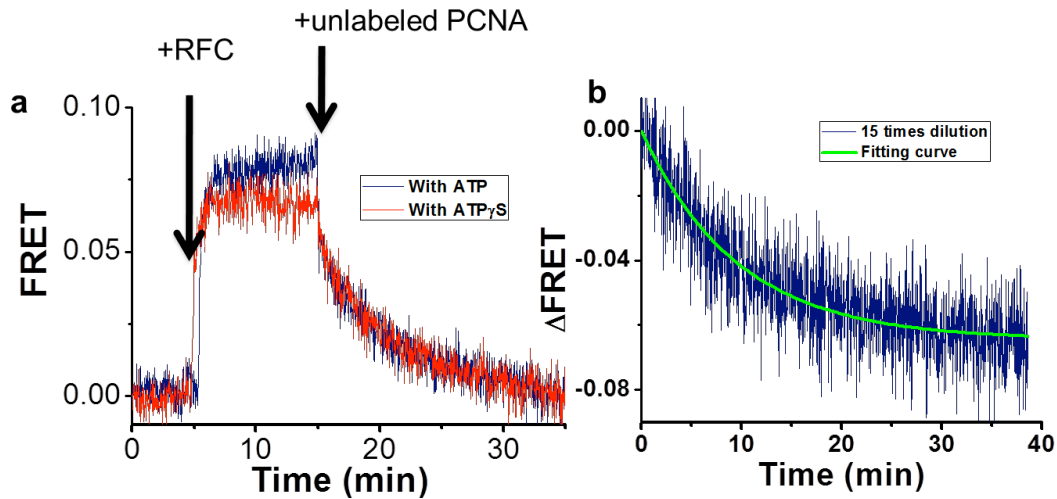


Supplementary Figure S3.

PCNA assembled by RFC exchanges with free PCNA in solution

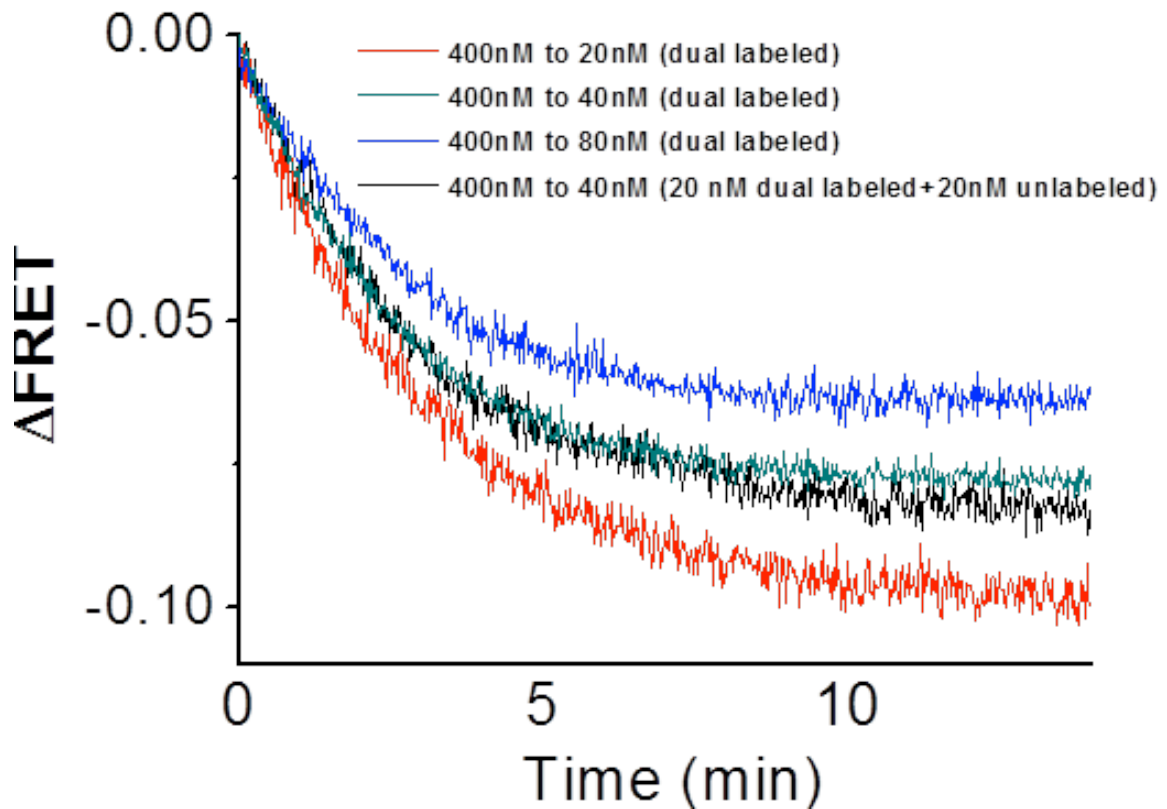
a. Rapid FRET increase between Cy3-PCNA (20 nM) and Cy5-PCNA (20 nM) upon addition of 1 mM ATP (or 1 mM ATP γ S) and 80 nM RFC. FRET decrease follows when 1 μ M unlabeled PCNA is added subsequently likely due to exchange with free PCNA in solution.

b. To rule out the possibility that the added unlabeled PCNA may induce the disassembly of the RFC-assembled PCNA trimer, we diluted the RFC-assembled PCNA trimer by a factor of 15 to a buffer solution while measuring FRET. The concentration before dilution is 20 nM Cy3 PCNA, 20 nM Cy5 PCNA, 1 mM ATP, 40 nM RFC. All experiments were done at 37 degree. To achieve 15 fold dilution, 25 μ l mixture was added into 350 μ l buffer. An exponential decay fit was used to determine the reaction time. Triple repeats were performed and yielded the average reaction time of 9.96 min with a standard deviation of 0.41 min.



Supplementary Figure S4.

Dissociation of Cy5/Cy3-PCNA trimers into monomers upon dilution. We pre-incubated 200 nM Cy3-PCNA and 200 nM Cy5-PCNA in solution at 37°C for 30 min to achieve equilibrium, and then diluted the mixture into a cuvette filled with buffer to investigate the FRET change. FRET measurements were also performed at 37°C. Different final FRET values are observed for different final concentrations. In one experiment, the dilution was made to 20 nM labeled PCNA plus 20 nM unlabeled PCNA. The data show that dilution results in FRET decrease over 3 min time scale, indicating that PCNA trimer spontaneously dissociates.

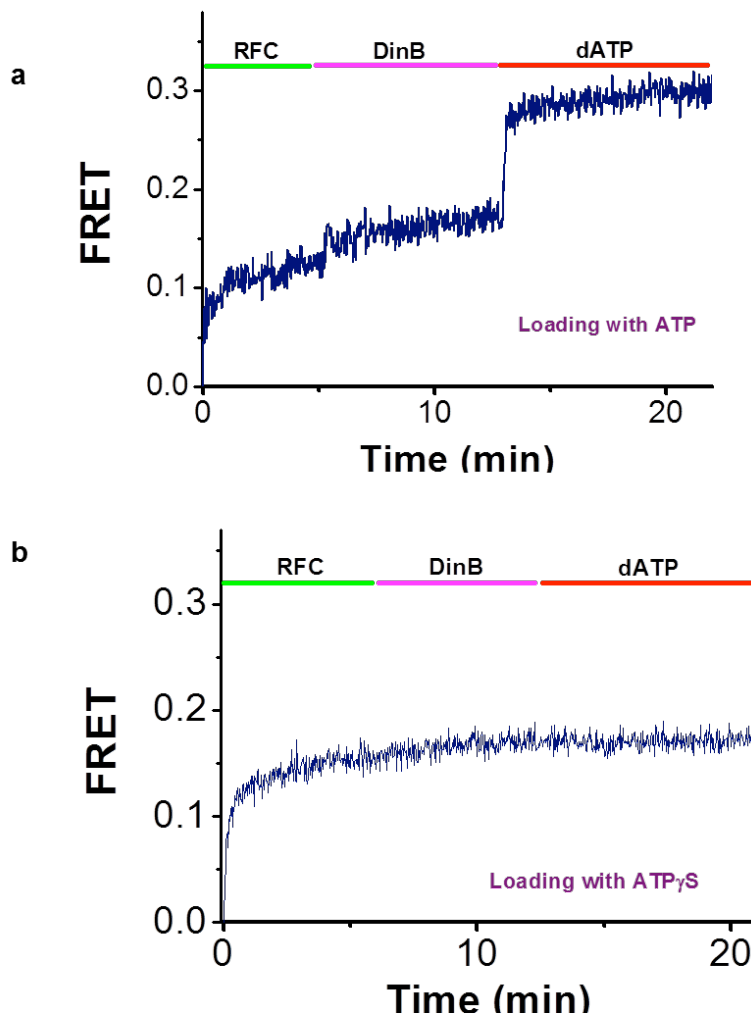


Supplementary Figure S5.

Movement of labeled PCNA during DNA synthesis by MacDinB requires ATP hydrolysis by MacRFC. The same experiments as shown in Figure 4 were performed using another batch of PCNA and RFC proteins.

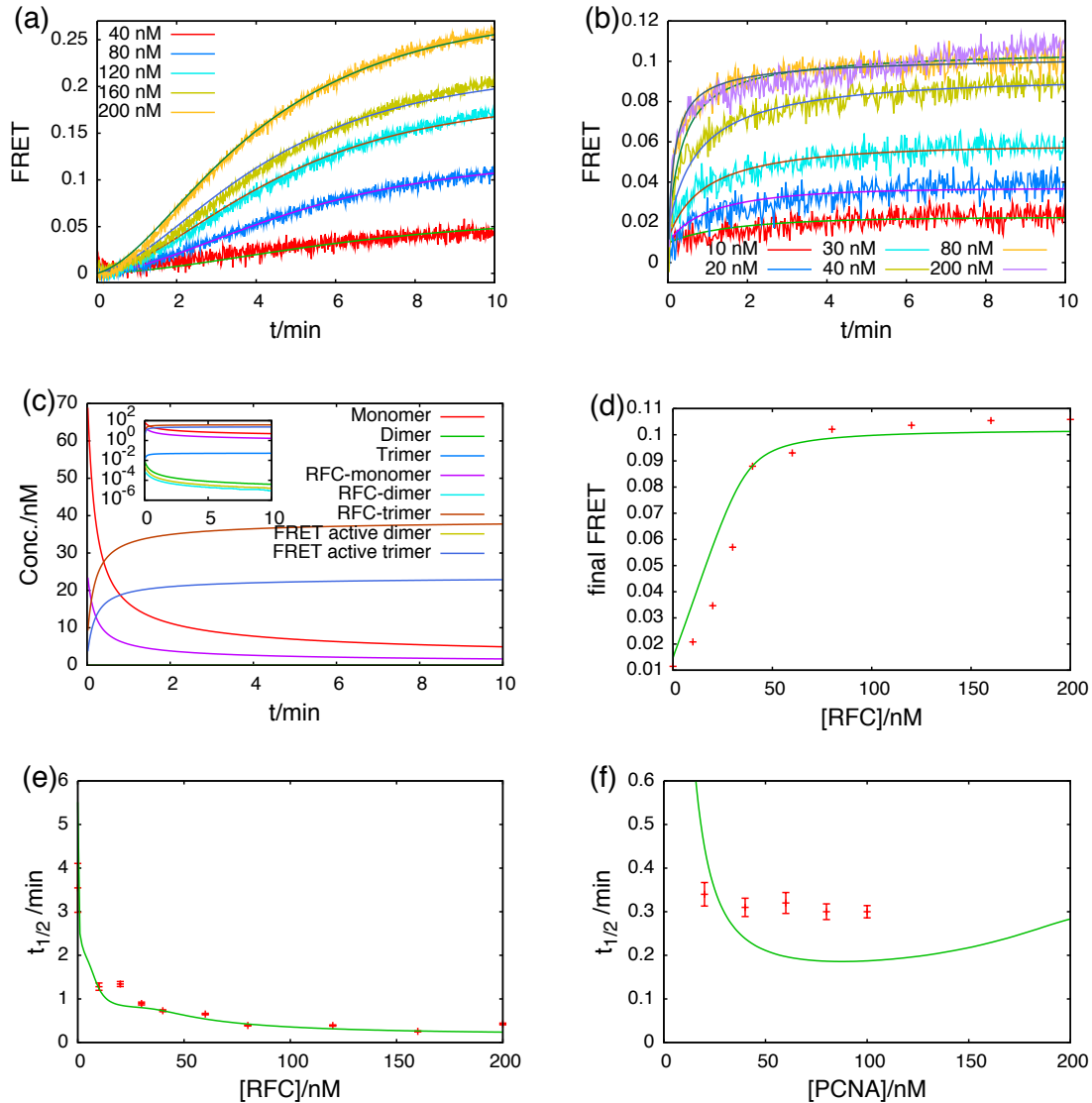
a. Addition of RFC (80nM) to the reaction mixture, which contained 1 mM ATP, leads to significant FRET increase due to Cy3-PCNA (20nM) loading onto the 4WJ-DNA (4WJ labeled) (50nM). DinB (2 μ M) addition followed by dATP (10 μ M) addition caused a significant jump in FRET.

b. In contrast, if 1 mM ATP γ S replaces ATP in the reaction, no FRET jump is observed showing the polymerization-dependent movement of PCNA requires the release of RFC from PCNA induced by ATP hydrolysis.



Supplementary Figure S6. Results of kinetic modeling of PCNA assembly dynamics.

The original data presented in Fig. 4 are shown along with the fits. **a.** Fit to assembly without RFC. **b.** Fit to RFC-assisted assembly. $[PCNA] = 40$ nM. **c.** Time evolution of various species at $[RFC] = 200$ nM, $[PCNA] = 40$ nM. Dimers expressed at a very low concentration as expected. **d.** Final FRET signal vs. $[RFC]$. **e.** Assembly half-time vs $[RFC]$. **f.** Assembly half-time vs $[PCNA]$.



Supplementary Table S1. The maximum FRET value attainable and the half lifetime of FRET increase during self-assembly of PCNA as a function of PCNA concentration. No significant FRET increase was observed at 10 nM PCNA and the maximum FRET value and the half lifetime were not determined (N.D.).

PCNA	Maximun FRET	Half-Life (min)
10nM	N.D.	N.D.
40nM	0.07	6.83
80nM	0.15	5.51
120nM	0.22	5.10
160nM	0.26	4.87
200nM	0.31	4.03
PCNA 40nM + RFC 100nM	0.34	0.32

Supplementary Table S2. Average decay time of the Cy3-PCNA/Cy5-PCNA FRET assembled in the absence of RFC or in the presence of RFC after adding unlabeled PCNA (1 μ M).

RFC	Cy3 PCNA	Cy5 PCNA	Decay Time (min)	Error (min)
none	100nM	100nM	6.6	0.1
none	80nM	80nM	6.9	0.1
none	60nM	60nM	8.2	0.2
none	40nM	40nM	6.7	0.2
RFC	Cy3 PCNA	Cy5 PCNA	Decay Time (min)	Error (min)
40nM	20nM	20nM	7.2	0.7
100nM	20nM	20nM	7.2	0.2
200nM	20nM	20nM	6.5	0.2

Supplementary Table S3: Computed rate constants obtained from fitting the kinetic modeling of PCNA assembly to the data

<i>Reaction</i>	<i>Parameter</i>	<i>Rate</i>	<i>Units</i>
$R + P \rightarrow RP$	k_o	2.5726	$nM^{-1} \text{min}^{-1}$
$RP \rightarrow R + P$	k'_o	1296.1	min^{-1}
$RP \rightarrow RP^*$	k_{act}	9.5028	min^{-1}
$RP^* \rightarrow RP$	k'_{act}	155.46	min^{-1}
$RP^* + P \rightarrow RP_2$	k_{aa}	25.349	$nM^{-1} \text{min}^{-1}$
$RP_2 \rightarrow RP^* + P$	k'_{aa}	8.8459×10^5	min^{-1}
$RP_2 + P \rightarrow RP_3$	k_{ab}	2478.5	$nM^{-1} \text{min}^{-1}$
$RP_3 \rightarrow RP_2 + P$	k'_{ab}	8.5213×10^{-7}	min^{-1}
$RP_3 \rightarrow R + P_3$	k_d	15.944	min^{-1}
$R + P_3 \rightarrow RP_3$	k'_d	71.678	$nM^{-1} \text{min}^{-1}$
$P + P \rightarrow P_2$	k_{ta}	1.3798	$nM^{-1} \text{min}^{-1}$
$P_2 \rightarrow P + P$	k'_{ta}	6.3889×10^5	min^{-1}
$P_2 + P \rightarrow P_3$	k_{tb}	0.9943	$nM^{-1} \text{min}^{-1}$
$P_3 \rightarrow P_2 + P$	k'_{tb}	0.21348	min^{-1}

Supplementary Table S4: Calibration constants. The average for self-assembly is $1.0089 \times 10^{-2} \text{ nM}^{-1}$ with range relative to the average of 1.61496. The average for assisted assembly is $4.8608 \times 10^{-3} \text{ nM}^{-1}$, with a relative range of 0.47071.

$[RFC]/\text{nM}$	$[PCNA]/\text{nM}$	$A/10^{-3} \text{ nM}^{-1}$
0	40	21.51
0	80	10.36
0	120	7.702
0	160	5.659
0	200	5.216
10	40	3.407
20	40	3.484
30	40	4.104
40	40	5.538
60	40	5.360
80	40	5.695
120	40	5.310
160	40	5.449
200	40	5.400